Snyder, A. P., Sudnick, D. R., Arkle, V.K., & Horrocks, W. DeW., Jr. (1981) *Biochemistry* (following paper in this issue).
Sowadsky, J., Cornick, G., & Kretsinger, R. H. (1978) *J. Mol. Biol. 124*, 123–132.
Sudnick, D. R. (1979) Ph.D. Thesis, The Pennsylvania State University, University Park, PA.
Thomas, D. D., Carlsen, W. F., & Stryer, L. (1978) *Proc. Natl. Acad. Sci. U.S.A. 75*, 5145–5750.
Woyski, M. M., & Harris, R. E. (1963) in *Treatise on Analytical Chemistry* (Kolthoff, I. M., & Elving, P. J., Eds.) Part 2, Vol. 8, p 58, Wiley, New York.
Yeh, S. M., & Meares, C. F. (1980) *Biochemistry 19*, 5057–5062.

Lanthanide Ion Luminescence Probes. Characterization of Metal Ion Binding Sites and Intermetal Energy Transfer Distance Measurements in Calcium-Binding Proteins. 2. Thermolysin†

A. Peter Snyder, Daniel R. Sudnick, Valerie K. Arkle, and William DeW. Horrocks, Jr.*

ABSTRACT: Eu(III) laser excitation spectroscopy of the $^7F_0 \rightarrow {}^5D_0$ transition reveals spectral features characteristic of the occupation of Eu(III) ions in the S(1), S(3), and S(4) Ca(II)-binding sites of thermolysin. Various hybrid Eu(III) thermolysin species were prepared in which the Eu(III) ion resides in the S(1) or S(3) and S(4) or all three Eu(III)-binding sites of the metalloprotein. The Eu(III) ion in the S(1) site coordinates to one H_2O molecule while the other two sites coordinate to about three to four H_2O molecules. Thermolysin hybrids in which the donor Ln(III) ion occupies S(1) and acceptor Ln(III) ions occupy sites S(3) and S(4) were prepared. Nonradiative energy transfer between Eu(III) and Tb(III) acting as luminescent donors and various other Ln(III) ions serving as acceptors was observed by monitoring the excited-state lifetimes of the donor ions using a pulsed dye laser apparatus. Virtually all energy transfer occurs between sites S(1) and S(4) while <1% of the donor's energy is transferred from S(1) to S(3). With the assumption of a Förster-type dipole–dipole mechanism, the experimental inter-binding-site distance estimates between sites S(1) and S(4) are in good agreement with the distance (11.7 Å) obtained by X-ray crystallography. R_0 values (critical distances for 50% energy transfer) in H_2O solution range from 9.3 Å for the Tb(III)–Ho(III) donor–acceptor pair down to 5.3 Å for the Eu(III)–Ho(III) pair.

In this, as in the preceding paper (Rhee et al., 1981), we seek to characterize the calcium-binding sites of a structurally well-characterized protein by using luminescence spectroscopic techniques developed in this laboratory (Horrocks & Sudnick, 1979a,b). Also we wish to establish the utility of the measurement of energy transfer between trivalent lanthanide ions, Ln(III), in determining distances between metal ion binding sites. Stryer (1978) and Steinberg (1971) have reviewed other types of energy-transfer distance measurement. Thermolysin (EC 3.4.24.4), a thermostable, calcium-binding zinc metalloendoprotease from *Bacillus thermoproteolyticus*, the subject of the present paper, is ideal for our purposes. Its amino acid sequence (Titani et al., 1972) and three-dimensional X-ray structure to a resolution of 2.3 Å (Matthews et al., 1972, 1974) have been determined. Moreover, a detailed study of the binding of Ln(III) ions at the calcium-binding sites, S(1), S(3), and S(4), has been carried out by using crystallographic techniques (Matthews & Weaver, 1974). The structural and functional roles of metal ions in thermolysin have recently been reviewed (Roche & Voordouw, 1978).

An earlier study by one of us (Horrocks et al., 1975) demonstrated by using ordinary fluorometry the occurrence of energy transfer between a luminescing Tb(III) occupying calcium site S(1) and an absorbing Co(II) substituted for Zn(II) at the active site of thermolysin. With the assumption of a Förster-type dipole–dipole mechanism (Förster, 1948, 1965), an estimate of the distance between Tb(III) and Co(II) of 13.7 Å was made, which was in good agreement with the distance between the Ca(II) ion in site S(1) and the active site Zn(II) ion found in the X-ray structure (Matthews et al., 1974). In the present study, energy transfer between emitting donor and absorbing acceptor Ln(III) ions occupying different calcium-binding sites is monitored via the reciprocal excited-state lifetimes of the luminescent donor ions using a pulsed dye laser excitation technique. This study is aided by the fact that it is possible to substitute selectively one type of Ln(III) ion, say Eu(III) in site S(1), and another type, say Nd(III), in sites S(3) and S(4).

Some uncertainty exists in the literature regarding the mechanism of inter-Ln(III)-ion energy transfer, e.g., whether it occurs by a dipole–dipole, dipole–quadrupole, or quadrupole–quadrupole mechanism (Reisfeld, 1975; Reisfeld, 1976; Nakazawa & Shionoya, 1967; Grant, 1971; Fong & Diestler, 1972). This research, which in effect uses a metalloprotein model to address this problem in photophysics, settles this controversy in favor of a dipole–dipole mechanism. Since our techniques are applicable to all states of matter, direct solution-state–solid-state comparisons can be made. A preliminary report of some of our findings has appeared elsewhere (Horrocks et al., 1980).

Materials and Methods

Materials. Thermolysin and deuterium oxide (99.7%) were purchased from Sigma Chemical Co. Ln(III) salts were obtained from either Research Organic/Inorganic or Alfa-

† From the Department of Chemistry, The Pennsylvania State University, University Park, Pennsylvania 16802. *Received July 24, 1980; revised manuscript received January 22, 1981.* Supported by Grant GM-23599 from the National Institute of General Medical Sciences, National Institutes of Health. Matching funds for the purchase of the departmental Mod-Comp computer and laser facilities were provided by the National Science Foundation.

0006-2960/81/0420-3334$01.25/0

Ventron Chemicals. All other chemicals were reagent grade or the purest commercially available.

Methods. Thermolysin was recrystallized by dissolving it in a 5 M NaBr, 10 mM $CaCl_2$, and 0.05 M Tris,[1] pH 6.0, buffer and dialyzing the sample to low ionic strength against the same buffer without NaBr. Enzyme concentrations were determined by measuring the absorbance at 280 nm (Beckman-Guilford spectrophotometer, Model 252) using $E_{1\%}^{280} = 17.65$ and a molecular weight of 34 600 (Ohta et al., 1966).

Preparation of Ln(III)-Substituted Derivatives. Tb[1]TL and Eu[1]TL. Recrystallized thermolysin was dissolved in a 0.05 M Tris buffer, pH 6.0, containing 5 M NaBr, 10 mM $CaCl_2$, and 1 equiv of Tb(III) or Eu(III) added as a solution of the chloride salt.

Tb[1,3,4]TL and Eu[1,3,4]TL. Recrystallized thermolysin crystals were soaked in a buffer [0.05 M Tris, pH 5.5, 0.01 M Ln(III) salt, and 5% (v/v) dimethyl sulfoxide] following the method of Matthews & Weaver (1974). The soaked crystals were then washed 3 times with deionized distilled water (DDW) and dissolved in a buffer: 5 M NaBr and 0.05 M Tris, pH 6.0, which was made 0.1 mM in either Tb(III) or Eu(III) to suppress dissociation from sites S(3) and S(4). Typical protein concentrations were in the 0.1–1.0 mM range for the laser experiments.

Hybrid Derivatives: Ln[1]Ln'[3,4]TL (Ln ≠ Ln'). A solution of Ln[1]TL dissolved in a 5 M NaBr, 10 mM $CaCl_2$, and 0.05 M Tris, pH 6.0, solution was recrystallized. These crystals were then soaked as described above in a buffer [0.05 M Tris, pH 5.5, 0.01 M Ln'(III) salt, and 5% (v/v) dimethyl sulfoxide]. The crystals were then washed with DDW and dried in vacuo which resulted in an opaque, pastelike protein mass for the solid-state experiments. For the solution-state experiments they were dissolved in a buffer (5 M NaBr, 0.05 M Tris, and 0.1 mM Ln'(III), pH 6.0).

Assay. The enzyme was assayed spectrophotometrically at 338 nm by using *N*-[3-(2-furyl)acryloyl]glycyl-L-leucinamide (FAGLA) (Feder, 1968) in a 0.05 M Tris buffer, pH 6.0, containing 0.1 M NaBr and 10 mM $CaCl_2$ at 25 °C. The Ln(III)-substituted thermolysin derivatives were found to have activities equal, within experimental error, to that of the native enzyme with k_{obsd}/E_0 values averaging 12.1×10^5 min^{-1} M^{-1}. Assays performed as above except with the NaBr concentration increased to 5 M had activities almost 10 times as great, $k_{obsd}/E_0 = 10.4 \times 10^6$ min^{-1} M^{-1}.

Visible absorption spectra of the various Ln(III) chelate complexes were obtained by using a Cary 17 spectrophotometer. The Ln(III) solutions were standardized by using arsenazo as indicator (Woyski & Harris, 1963). Absorption and emission spectra were digitized and spectral overlap integrals calculated by using a Mod-Comp II/25 computer system.

Emission spectra were obtained with a Perkin-Elmer MPF-44A spectrofluorometer equipped with a differential corrected spectra microprocessor unit, which was checked with a solution of anthracene in ethanol and was found to agree within 2% of the published spectrum (Berlman, 1965; Drushel et al., 1963). Sensitized emission of Tb(III) and Eu(III) bound to thermolysin was observed with excitation at 295 nm.

Luminescence lifetimes of Eu(III) and Tb(III) and Eu(III) excitation spectra were obtained by using an apparatus described elsewhere (Sudnick, 1979). Eu(III) and Tb(III) ions were excited in the 579- and 488-nm regions, respectively. Identical optical arrangements were used for the solution- and solid-state measurements. No special precautions were necessary to eliminate scattered light in the latter case.

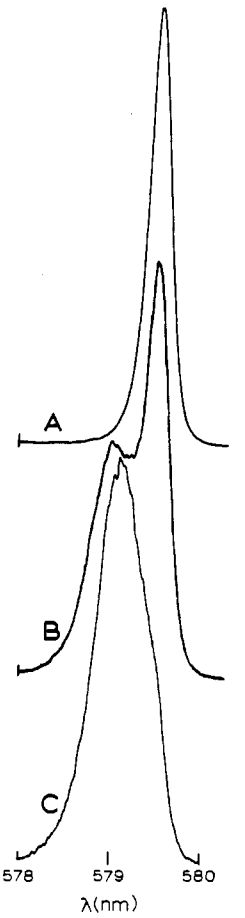

FIGURE 1: Characteristic $^7F_0 \rightarrow {}^5D_0$ excitation spectra of Eu(III) in the (A) S(1) site, (B) S(1), S(3), and S(4) sites, and (C) S(3) and S(4) metal-binding sites.

Results

Characterization of Ln(III) Ion Binding via $^7F_0 \rightarrow {}^5D_0$ Eu(III) Excitation Spectroscopy. The $^7F_0 \rightarrow {}^5D_0$ excitation spectrum of a solution of Eu[1]TL (Figure 1A) consists of a single sharp Lorentzian peak at 579.5 nm with a width at half-height of 0.3 nm. It can confidently be attributed to a species with a Eu(III) ion occupying calcium site S(1) (Matthews & Weaver, 1974). The corresponding excitation spectrum of Eu[1,3,4]TL prepared according to the method of Matthews & Weaver (1974) is shown in Figure 1B. Additional features on the high-energy side are attributable to Eu(III) ions occupying sites S(3) and S(4). Titration of native thermolysin with Eu(III) beyond 1 equiv produces excitation spectra showing these high-energy features, but the intensity of these features never equals that obtained by the crystal-soaking procedure, no matter how much Eu(III) is added to solution.

That Eu(III) bound at S(1) is virtually exchange inert is shown by the following experiment. Dy[1]Eu[3,4]TL was prepared as described earlier and its excitation spectrum recorded (Figure 1C). The feature at 579.5 nm characteristic of Eu(III) in site S(1) is virtually absent; only a feature centered at 579.1 nm characteristic of Eu(III) in sites S(3) and S(4) is evident. This result demonstrates that it is possible to synthesize hybrid Ln(III)-substituted species which are

[1] Abbreviations used: DPA, 2,6-pyridinedicarboxylic acid; Ln[1]TL, Ln(III) ion substituted at Ca(II) site S(1) of thermolysin with Ca(II) ions remaining at sites S(3) and S(4); Ln[1,3,4]TL, Ln(III) ions substituted at Ca(II) sites S(1), S(3), and S(4); Ln[1]Ln'[3,4]TL, Ln(III) at site S(1) and Ln'(III) at sites S(3) and S(4); Tris, tris(hydroxymethyl)aminomethane.

Table I: Reciprocal Excited State Lifetimes, τ^{-1}, Energy-Transfer Efficiencies, E, Spectral Overlap Integrals, J, Critical Distances for 50% Energy Transfer, R_0, and the Experimentally Estimated Distances, r, between Sites S(1) and S(4) of Thermolysin for Various Donor-Acceptor Ln(III) Ion Pairs[a]

donor	acceptor	state	τ^{-1} (ms^{-1})	E[b]	J ($\times 10^{18}$ cm^6 mol^{-1})[c]	R_0 (Å)[d]	r (Å)[e]
Eu(III)	Pr(III)	solution	1.98	0.101	6.50	8.20	11.8
Eu(III)	Pr(III)	solid	2.07	0.111	6.50	8.20	11.6
Eu(III)	Nd(III)	solution	2.12	0.160	8.26	8.53	11.2
Eu(III)	Nd(III)	solid	2.21	0.167	8.26	8.53	11.2
Tb(III)	Pr(III)	solution	0.78	0.115	2.66	7.77	10.9
Tb(III)	Pr(III)	solid	0.84	0.107	2.66	7.77	11.1
Tb(III)	Nd(III)	solution	1.62	0.587	6.95	9.12	8.6
Tb(III)	Nd(III)	solid	1.67	0.551	6.95	9.12	8.8
Tb(III)	Ho(III)	solution	0.89	0.225	7.93	9.33	11.5
Tb(III)	Ho(III)	solid	1.04	0.279	7.93	9.33	10.9
Tb(III)	Er(III)	solution	0.80	0.138	3.39	8.09	11.0
Tb(III)	Er(III)	solid	0.85	0.122	3.39	8.09	11.2

[a] All symbols are as defined in Horrocks et al. (1980). [b] $E = 1 - (\tau/\tau_0)$. [c] $J = \int F(\nu)\epsilon(\nu)\nu^{-4}\, d\nu / \int F(\nu)\, d\nu$; calculated by using absorption spectra of $[Ln^{III}(DPA)_3]^{3-}$ complexes. [d] $R_0^6 = (8.78 \times 10^{-25})\kappa^2\phi n^{-4}J$ with $\kappa^2 = 2/3$, $n^{-4} = 0.294$, $\phi_{Eu} = 0.27$, and $\phi_{Tb} = 0.48$. [e] $r = R_0[(1-E)/E]^{1/6}$.

important to our energy-transfer experiments.

Determination of the Number of Water Molecules, q, Coordinated at Various Sites. The reciprocal lifetime, τ^{-1}, values for excitation into the sharp signal at 579.5 nm of Eu[1]TL are $\tau_{H_2O}^{-1} = 1.78$ ms^{-1} and $\tau_{D_2O}^{-1} = 0.61$ ms^{-1} in H_2O and D_2O solution, respectively. Using eq 1 (Horrocks & Sudnick,

$$q_{Eu} = 1.05(\tau_{H_2O}^{-1} - \tau_{D_2O}^{-1}) \quad (1)$$

1979b) the number of coordinated water molecules, q, is found to be 1.2 ± 0.5. The results for excitation into the same band of Eu[1,3,4]TL are $\tau_{H_2O}^{-1} = 1.83$ ms^{-1} and $\tau_{D_2O}^{-1} = 0.65$ ms^{-1} yielding an identical value of $q = 1.2 \pm 0.5$. Excitation of the feature at 579.1 nm of Eu[1,3,4]TL or Dy[1]Eu[3,4]TL yielded exponential decay curves in H_2O solution that could be resolved into separate components with average τ^{-1} values of 4.86 and 3.98 ms^{-1}. In D_2O solution only a single exponential of $\tau_{D_2O}^{-1} = 1.00$ ms^{-1} was observed. These results lead (by using eq 1) to q values of 4.0 and 3.1.

In the case of Tb[1]TL the excitation spectrum ($^7F_6 \rightarrow {}^5D_4$) consists of a single feature centered at 490.5 nm with a width at half-height of 5.15 nm. The reciprocal lifetime results for excitation into this band are $\tau_{H_2O}^{-1} = 0.69$ ms^{-1} and $\tau_{D_2O}^{-1} = 0.41$ ms^{-1} which, by using eq 2 (Horrocks & Sudnick, 1979a),

$$q_{Tb} = 4.2(\tau_{H_2O}^{-1} - \tau_{D_2O}^{-1}) \quad (2)$$

yield $q = 1.2 \pm 0.5$, in good agreement with the Eu(III) results. In the case of Tb(III) both the ground ($^7F_6$) and excited ($^5D_4$) states are split by the ligand field and selective excitation of Tb(III) in the individual sites is not possible. Luminescence decay curves obtained on solutions of Tb[1,3,4]TL are not simple exponentials.

Energy Transfer from Eu(III) or Tb(III) to Other Ln(III) Ions. Since it is demonstrably possible to synthesize hybrids with one type of Ln(III) ion at site S(1) and another type at sites S(3) and S(4), our experiments were carried out with a donor Eu(III) or Tb(III) in site S(1) and various other Ln(III) acceptor ions in the other sites. The reciprocal excited-state lifetimes of Eu(III) and Tb(III) in the various hybrid substituted thermolysin samples are given in Table I for both solutions and crystals. Reciprocal lifetime values in the absence of energy transfer (τ_0^{-1}) were obtained from hybrids involving nonacceptor ions in sites S(3) and S(4). With Eu(III) as the donor, the following series of nonacceptor ions, Ca(II), La(III), Ce(III), Gd(III), Dy(III), Tm(III), Yb(III), and Lu(III), gave solution-state $\tau_{H_2O}^{-1}$ values as follows: 1.78, 1.75, 1.74, 1.75, 1.80, 1.82, 1.78, and 1.78 ms^{-1}, respectively. In the same order with Tb(III) as the donor, the solution-state $\tau_{H_2O}^{-1}$ values were as follows: 0.69, 0.70, 0.70, 0.71, 0.71, 0.73, 0.71, and 0.72 ms^{-1}. Solution-state $\tau_{D_2O}^{-1}$ values of 0.61 and 0.41 ms^{-1} were obtained for Eu[1]TL and Tb[1]TL, respectively. In the solid-state the values $\tau_{H_2O}^{-1} = 1.85$ and 0.75 ms^{-1} and $\tau_{D_2O}^{-1} = 0.72$ and 0.46 ms^{-1} for Eu[1]TL and Tb[1]TL, respectively, were found.

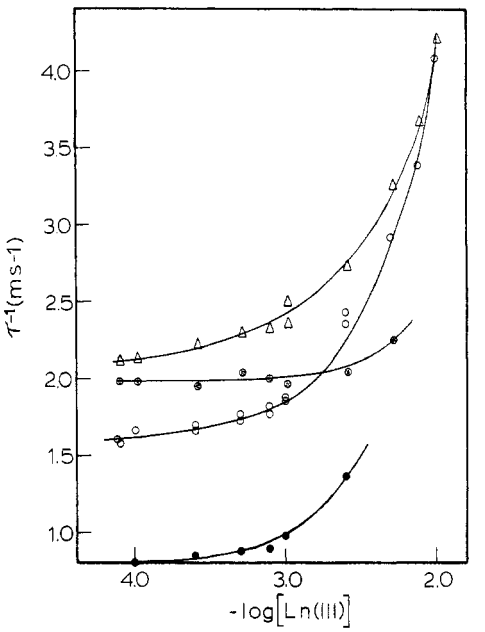

FIGURE 2: Effect of excess, free Ln(III) on the reciprocal lifetime values, τ^{-1}, of Tb[1]Er[3,4]TL (●), Tb[1]Nd[3,4]TL (○), Eu[1]-Pr[3,4]TL (⊛), and Eu[1]Nd[3,4]TL (△).

The solution-state τ^{-1} values for the energy-transfer measurements were made on solutions containing a slight excess of acceptor ion in solution in order to suppress the dissociation of these ions from sites S(3) and S(4). The possibility that this quantity (~0.1 mM) of free acceptor Ln(III) ions could affect the lifetime results by collisional deexcitation was explored. Reciprocal lifetime measurements were made on solutions of Eu[1]Pr[3,4]TL, Eu[1]Nd[3,4]TL, Tb[1]Er[3,4]-TL, and Tb[1]Nd[3,4]TL as a function of free Ln(III) acceptor ion [Ln(III) = Pr(III), Nd(III) or Er(III)] in solution. Those results are shown in Figure 2. It is clear that at free Ln(III) ion concentrations >1 mM significant collisional quenching occurs; however, at a free Ln(III) ion concentration of 0.1 mM or lower the τ^{-1} values become constant suggesting that collisional quenching is unimportant in this region. The solution-state τ^{-1} values reported in Table I were obtained under the latter conditions. Experiments at various thermolysin concentrations in the range 0.1–1 mM show no difference, within experimental error, in the measured τ^{-1} values, suggesting that interprotein energy transfer is unimportant at these concentrations.

Quantum Yields. The ratio of excited-state lifetimes in H_2O and D_2O solution, τ_{H_2O}/τ_{D_2O}, provides an upper-limit estimate of the quantum yield, ϕ [0.59 and 0.34 for Tb(III) and Eu(III), respectively], in site S(1) of thermolysin. The true values are undoubtedly somewhat less. For Eu(III) a value decreased by 21% was chosen. For Tb(III), emission experiments using the 488-nm line of an argon ion laser as the excitation source

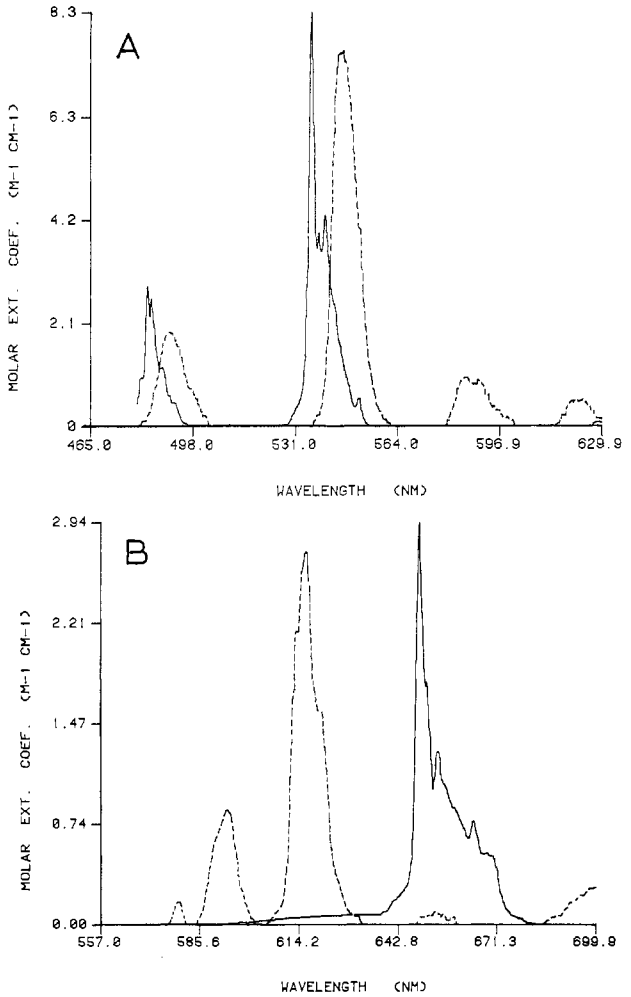

FIGURE 3: Spectral overlap plots of protein-bound emission and acceptor absorption. (A) Tb(III) emission and $[Ho^{III}(DPA)_3]^{3-}$ absorption; (B) Eu(III) emission and $[Er^{III}(DPA)_3]^{3-}$ absorption.

and an aqueous $TbCl_3$ solution as a standard gave ϕ_{Tb} values of 0.36 and 0.60, depending on whether the quantum yield of the standard was taken as 0.046 (Dawson et al., 1966) or 0.084 (Stein & Wurzberg, 1975). For these quantum yield estimates the average molar extinction coefficient at the 488-nm line of a series of model chelate complexes (0.0688 M^{-1} cm^{-1}) was employed. An average ϕ_{Tb} value of 0.48 is used in our analysis.

Emission and Absorption Spectra. The emission spectra of Tb(III) and Eu(III) bound at site S(1) of thermolysin, necessary to the calculation of the spectral overlap integrals, J (see the footnotes to Table I for the equations used in the Förster energy-transfer analysis), are shown in parts A and B, respectively, of Figure 3. Also required are the absorption spectra of the protein-bound acceptor ions; however, owing to their low molar extinction coefficients these spectra are unavailable. The spectra of model complexes must be used instead. As in our parvalbumin study (Rhee et al., 1981), we have chosen to use the absorption spectra of the model $[Ln^{III}(DPA)_3]^{3-}$ complexes to evaluate the spectral overlap integrals. Absorption spectra for such complexes of Nd(III) and Pr(III) are given in Rhee et al. (1981). Figure 3 shows the absorption spectra of the corresponding Ho(III) and Er(III) complexes. None of the other Ln(III) ions show appreciable absorption in the region of Eu(III) and Tb(III) emission so that their J integrals are effectively 0. Absorption spectra were recorded on a variety of aminopolycarboxylate chelate complexes. The J overlap integrals evaluated from these spanned a modest range (Horrocks et al., 1980), leading to some uncertainty in the estimated R_0 values. The J values calculated by using the absorption spectra of $[Ln^{III}(DPA)_3]^{3-}$ complexes are listed in Table I along with the R_0 values derived therefrom.

Nakazawa & Shionoya (1967) have reported R_0 values in conjunction with their study of inter-Ln(III)-ion energy transfer in glasses. For instance, they report R_0 values for the donor–acceptor pairs, Tb(III) → Nd(III), 12.4 Å, Tb(III) → Ho(III), 11.6 Å, and Tb(III) → Er(III), 10.3 Å, which are somewhat larger than the corresponding R_0 values calculated by us (Table I). Using their published absorption and emission spectra (suitably enlarged), we have calculated R_0 values (ϕ = 1.0, n = 1.59, $\kappa^2 = {}^2/_3$) with the following results: 10.4, 9.5, and 8.6 Å for the above-mentioned donor–acceptor pairs in the same order. The latter values are much more in line with those that we obtained by using the absorption spectra of our model complexes.

Discussion and Analysis

Characterization of Metal Ion Binding Sites. Observation of the $^7F_0 \rightarrow {}^5D_0$ transition of a Eu(III) ion bound to a protein by excitation spectroscopy (Horrocks & Sudnick, 1979b) provides an unambiguous characterization of the binding sites. Since this transition occurs between nondegenerate levels, ligand field splitting is impossible and a single Eu(III) ion environment will produce a single peak in the excitation spectrum. The excitation spectrum of Eu[1]TL (Figure 1A) consists of a single narrow Lorentzian peak at 579.5 nm while the spectrum of Eu[1,3,4]TL exhibits additional features at higher energy characteristic of Eu(III) ions in sites S(3) and S(4). Sudnick (1979) has noted a rough linear correlation of the energy of the $^7F_0 \rightarrow {}^5D_0$ transition with the total charge on Eu(III) complexes. For instance, in $[Eu^{III}(DPA)_3]^{3-}$ this transition occurs at 17231 cm^{-1} while for the aqua ion, Eu^{3+}_{aq}, it occurs at 17272 cm^{-1}. The present results on thermolysin are in accord with this correlation since site S(1), with the lowest energy $^7F_0 \rightarrow {}^5D_0$ transition, involves the coordination of four carboxyate groups (Asp-138, Glu-177, Asp-185, Glu-190) while S(3) involves two carboxylate groups (Asp-57, Asp-59) and S(4) involves only one (Asp-200).

The excitation signals corresponding to the individual Eu(III) binding sites may be further characterized by their excited-state lifetimes which, when measured in both H_2O and D_2O, provide a direct measure of the number of metal-coordinated water molecules (Horrocks & Sudnick, 1979a). Our finding that Eu(III) bound at site S(1) has 1.2 ± 0.5 coordinated water molecules is consistent with the X-ray structural result on the native protein (Matthews & Weaver, 1974) that one water molecule is coordinated there, although some reorganization of this site can be expected upon expulsion of the Ca(II) ion from S(2). The lifetime experiments with Tb(III) lead to the same result. The luminescence decay experiments for Eu(III) ions occupying sites S(3) and S(4) are more ambiguous owing to the biphasic nature of the decay curves which, however, suggest about 3.1 and 4.0 coordinated water molecules. In accord with this finding the X-ray results (Matthews & Weaver, 1974) show that Eu(III) at S(3) involves 3 coordinated water molecules, as does Eu(III) at S(4) which has a coordinated threonine hydroxyl as well, worth, in this regard, approximately half a water molecule for a total of 3.5 [see Rhee et al. (1981)].

Ln(III) ions bound at site S(1) are exchange inert. This is demonstrated by the fact that when Dy[1]TL is crystallized and then soaked in a buffer containing 10 mM Eu(III), the Eu(III) excitation spectrum (Figure 1C) shows signals characteristic of Eu(III) in sites S(3) and S(4), but the absence

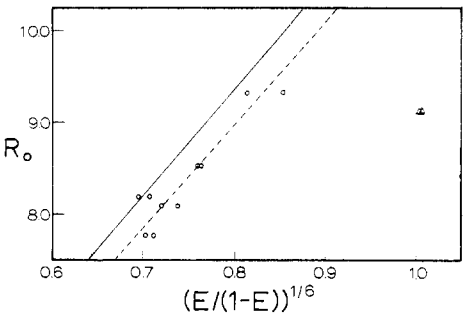

FIGURE 4: Plot of R_0 vs. $[E/(1-E)]^{1/6}$ of Tb-Nd (Δ) and other Ln-Ln′ (O) hybrids. The theoretical slope of 11.7 Å is shown as a solid line, and the least-squares slope (excluding the Tb–Nd pairs) appears as a dashed line.

of a peak at 579.5 nm shows that there is virtually no Eu(III) in site S(1). The exchange inertness of the S(1) site allows the synthesis of hybrid species, such as Eu[1]Nd[3,4]TL, which facilitate the energy-transfer experiments.

Energy-Transfer Distance Measurements. Hybrid species with a donor Eu(III) or Tb(III) ion at S(1) and various acceptor ions at sites S(3) and S(4) were synthesized. The crystal structure (Matthews et al., 1974) shows the S(1) to S(4) distance to be 11.7 Å while the S(1) to S(3) separation is 29.6 Å. Owing to the r^{-6} dependence of Förster-type energy transfer, the S(1) to S(3) energy transfer will amount to <1% of the S(1) to S(4) energy transfer, so the former can safely be neglected. Dissimilar ions occupying sites S(1) and S(4) are, in effect, an isolated donor–acceptor pair. In order to avoid complications due to an isolated donor ion at site S(3), we carried out all energy-transfer experiments with the donor ion at site S(1) and acceptor ions at sites S(3) and S(4).

The energy-transfer results (Table I) reveal measurable transfer efficiencies for those donor–acceptor pairs for which sizable J overlap integrals are calculated. With the exception of the Tb(III) → Nd(III) pair, the efficiencies correlate well with the magnitude of the J integrals and the R_0 values calculated therefrom (vide infra). In the cases of nonacceptor ions where the J integrals vanish no energy transfer was observed, nor was energy transfer detected in the cases of the Eu(III)–Ho(III) and Eu(III)–Er(III) pairs where quite small J values of 0.48×10^{-18} and 0.61×10^{-18} cm^6 mol^{-1}, respectively, were calculated (leading to R_0 values of 5.3 and 5.5 Å, respectively).

For reasons described elsewhere (Rhee et al., 1981), R_0 values were calculated with J integrals computed by using the absorption spectra of model complexes, a source of some uncertainty. The orientation factor, κ^2, was taken as $^2/_3$, and for the refractive index, n, a value of 1.35 was chosen (Rhee et al., 1981).

Taking the calculated R_0 values and the measured energy-transfer efficiencies, we obtained the values of the donor–acceptor separation, r, listed in Table I. With the exception of the Tb(III) → Nd(III) pair, the r values are in good agreement with the S(1) to S(4) separation of 11.7 Å found in the X-ray structure (Matthews et al., 1974). The equation given in footnote *e* of Table I can be rearranged to give eq 3

$$R_0 = r[E/(1-E)]^{1/6} \quad (3)$$

which allows a graphical analysis of the energy-transfer data. In Figure 4 the R_0 values are plotted vs. the quantity $[E/(1-E)]^{1/6}$. Equation 3 predicts a linear plot passing through the origin with a slope equal to the actual donor–acceptor separation, r. Taking both the solid- and solution-state data, but omitting the Tb(III) → Nd(III) results (triangles), we found that the best least-squares fit (dashed line) has a slope of 11.2 (3) Å (the standard deviation of the least significant figure is given in parentheses) and an intercept on the y axis of 0.0 (2) Å with a linear correlation coefficient (lcc) of 0.997. The theoretical line for r = 11.7 Å is also shown on the plot (solid line), and the agreement is good.

Our laser techniques are equally applicable to the solution and solid states and provide a spectroscopic structural probe which allows a direct comparison between the two states. When the least-squares analysis was applied individually to the solution- and solid-state data, the following results were obtained. The solution data give the following results: slope r = 11.3 (4) Å; y intercept = 0.0 (3) Å; lcc = 0.998. These results are in excellent agreement with the expectations from the crystal structure. The solid-state data give the following results: slope r = 11.1 (2) Å, y intercept = 0.0 (2) Å, lcc = 0.999. These results imply that the distance between sites S(1) and S(3) is not significantly altered upon dissolution of thermolysin.

Taken all together the satisfactory agreement between our energy-transfer distance measurements and the solid-state X-ray results justifies our initial assumption of a dipole–dipole mechanism for inter-Ln(III)-ion energy transfer. Our findings would appear to settle the controversy over the multipolar nature of the mechanism which was alluded to in the introduction. The protein thermolysin allows one, in effect, to isolate a pair of Ln(III) ions (the theoretically treated case), whereas experiments with doped glasses and single crystals have potential multibody interactions as a complicating factor (Grant, 1971; Fong & Diestler, 1972). Why the Tb(III) → Nd(III) pair appears to exhibit more energy transfer than expected from our analysis is not known. It may be related to the fact that the acceptor transition ($^4G_{5/2} \leftarrow {}^4I_{1/2}$) which is chiefly responsible for the spectral overlap is "hypersensitive" (Jorgensen & Judd, 1964), leading to an underestimation of the J overlap integral or, less likely, to some contribution from a dipole–quadrupole mechanism. It would appear, excepting perhaps the Tb(III) → Nd(III) case, that inter-Ln(III)-ion energy transfer provides a valid measure of distance between metal binding sites and is a useful addition of the spectroscopic arsenal of the molecular biologist.

References

Berlman, I. B. (1965) *Handbook of Fluorescence Spectra of Aromatic Molecules*, p 123, Academic Press, New York.

Dawson, W. R., Kropp, J. L., & Windsor, M. W. (1966) *J. Chem. Phys. 45*, 2410–2418.

Drushel, H. V., Sommers, A. L., & Cox, R. C. (1963) *Anal. Chem. 35*, 2166–2172.

Feder, J. (1968) *Biochem. Biophys. Res. Commun. 32*, 326–332.

Fong, F. K., & Diestler, D. J. (1972) *J. Chem. Phys. 56*, 2875–2880.

Förster, Th. (1948) *Ann. Phys. (Leipzig) 2*, 55–75.

Förster, Th. (1965) in *Modern Quantum Chemistry* (Sinanoglu, O., Ed.) Part 2, pp 93–137, Academic Press, New York.

Grant, W. J. C. (1971) *Phys. Rev. B: Solid State 4*, 648–663.

Horrocks, W. DeW., Jr., & Sudnick, D. R. (1979a) *J. Am. Chem. Soc. 101*, 334–340.

Horrocks, W. DeW., Jr., & Sudnick, D. R. (1979b) *Science (Washington, D.C.) 206*, 1194–1196.

Horrocks, W. DeW., Jr., Holmquist, B., & Vallee, B. (1975) *Proc. Natl. Acad. Sci. U.S.A. 72*, 4764–4768.

Horrocks, W. DeW., Jr., Rhee, M.-J., Snyder, A. P., & Sudnick, D. R. (1980) *J. Am. Chem. Soc. 102*, 3650–3652.

Jorgensen, C. K., & Judd, B. R. (1964) *Mol. Phys. 8*, 281–290.
Matthews, B. W., & Weaver, L. H. (1974) *Biochemistry 13*, 1719–1725.
Matthews, B. W., Colman, P. M., Jansonius, J. N., Titani, K., Walsh, K. A., & Neurath, H. (1972) *Nature (London), New Biol. 238*, 41–43.
Matthews, B. W., Weaver, L. H., & Kester, W. R. (1974) *J. Biol. Chem. 249*, 8030–8044.
Nakazawa, E., & Shionoya, S. (1967) *J. Chem. Phys. 47*, 3211–3219.
Ohta, Y., Ogura, Y., & Wada, A. (1966) *J. Biol. Chem. 241*, 5919–5925.
Reisfeld, R. (1975) *Struct. Bonding (Berlin) 22*, 123–174.
Reisfeld, R. (1976) *Struct. Bonding (Berlin) 30*, 65–98.
Rhee, M.-J., Sudnick, D. R., Arkle, V. K., & Horrocks, W. DeW., Jr. (1981) *Biochemistry* (preceding paper in this issue).
Roche, R. S., & Voordouw, G. (1978) *CRC Crit. Rev. Biochem. 5*, 1–23.
Stein, G., & Wurzberg, E. (1975) *J. Chem. Phys. 62*, 208–213.
Steinberg, I. Z. (1971) *Annu. Rev. Biochem. 40*, 83–114.
Stryer, L. (1978) *Annu. Rev. Biochem. 47*, 819–846.
Sudnick, D. R. (1979) Ph.D. Thesis, The Pennsylvania State University, University Park, PA.
Titani, K., Hermodson, M. A., Ericsson, L. H., Walsh, K. A., & Neurath, H. (1972) *Nature (London), New Biol. 238*, 35–37.
Woyski, M. M., & Harris, R. E. (1963) in *Treatise on Analytical Chemistry* (Kolthoff, I. M., & Elving, P. J., Eds.) Part 2, Vol. 8, p 58, Wiley, New York.

Resonance Raman and Absorption Spectroscopic Detection of Distal Histidine–Fluoride Interactions in Human Methemoglobin Fluoride and Sperm Whale Metmyoglobin Fluoride: Measurements of Distal Histidine Ionization Constants†

Sanford A. Asher,* Mary L. Adams, and Todd M. Schuster

ABSTRACT: The pH dependence of the resonance Raman and absorption spectra of human methemoglobin fluoride ($Hb^{III}F$) and sperm whale metmyoglobin fluoride ($Mb^{III}F$) has been examined. Both the Raman and absorption spectra of $Hb^{III}F$ and $Mb^{III}F$ indicate the existence at alkaline pH of an equilibrium between the hydroxide and fluoride complexes. The absorption maxima of $Hb^{III}F$ and $Mb^{III}F$ solutions shift to longer wavelengths as the pH is decreased from neutrality. The Raman data show a corresponding shift of the 461- and 468-cm^{-1} Fe–F vibrational stretching peaks at pH 7.0 [Asher, S. A., & Schuster, T. M. (1979) *Biochemistry 18*, 5377] to 399 and 407 cm^{-1} at acid pH in $Mb^{III}F$ and $Hb^{III}F$, respectively. These shifts are interpreted to result from protonation of the distal histidine and the formation of a hydrogen bond to the fluoride ligand. Measurements of the pH dependence of the absorption and resonance Raman spectra give distal histidine ionization constants (apparent) corresponding to pK = 5.1 (±0.1) for $Hb^{III}F$ and pK = 5.5 (±0.1) for $Mb^{III}F$. An examination of the distal histidine pK values and the frequency of the hydrogen-bonded Fe–F stretching vibration at pH 5.0 of $Hb^{III}F$ with and without inositol hexaphosphate indicates little difference in the distal histidine–heme distance between the so-called R and T quaternary forms of $Hb^{III}F$. These results indicate that the changes in the electronic spectrum of $Hb^{III}F$ that occur upon switching from the R to the T form do not result from alterations in (1) the iron–fluoride bond distance, (2) the iron out-of-heme plane distance, or (3) the distal histidine–fluoride distance.

Hemoglobin cooperativity depends upon the modulation of heme–ligand affinity by the globin portion of the molecule in response to binding at other sites on the protein. One approach that has been taken to elucidate the mechanism of cooperativity in hemoglobin has been to study the structural changes in the ferric derivatives of hemoglobin which are brought about by the binding of allosteric effectors [for recent reviews, see Perutz (1979) and Moffat et al. (1979)]. The quaternary structure of methemoglobin fluoride ($Hb^{III}F$)[1] is that of the liganded ferrous derivative, the so-called "R structure" (Deatherage et al., 1976), whereas in the presence of inositol hexaphosphate ($InsP_6$) it assumes the "T structure" of deoxyhemoglobin (Fermi & Perutz, 1977). This structural change gives rise to changes in SH reactivity and UV, visible, CD, and proton NMR spectra (Perutz et al., 1974a–c, 1978) which appear to be diagnostic for similar R–T conversions in other hemoglobin derivatives.

In an effort to define this R–T structural change in terms of bonding changes, we have used resonance Raman spectroscopy to study accompanying changes of iron spin state, iron–axial ligand bonding, and heme geometry (Asher et al., 1977; Asher & Schuster, 1979, 1981a,b). A central conclusion of those studies was that the iron–fluoride bond distance does not change when methemoglobin fluoride is switched from the R to the T conformation. Here, we report on an examination

† From the Gordon McKay Laboratory, Division of Applied Sciences, Harvard University, Cambridge, Massachusetts 02138 (S.A.A.), and the Biochemistry and Biophysics Section, Biological Sciences Group, University of Connecticut, Storrs, Connecticut 06268 (M.L.A. and T.M.S.). *Received November 12, 1980.* This work was supported by National Institutes of Health Grants GM-24081 (to P. S. Pershan) and HL-24644 and National Science Foundation Grant PCM 79-03964 (to T.M.S.).
* Address correspondence to this author at the Department of Chemistry, University of Pittsburgh, Pittsburgh, PA 15260.

[1] Abbreviations used: $Hb^{III}F$, methemoglobin fluoride; $Mb^{III}F$, metmyoglobin fluoride; $InsP_6$, inositol hexaphosphate; Hepes, *N*-2-(hydroxyethyl)piperazine-*N*′-2-ethanesulfonic acid.

0006-2960/81/0420-3339$01.25/0